# Syntheses, Crystal Structures, Magnetic Properties, and EPR Spectra of Tetranuclear Copper(II) Complexes Featuring Pairs of "Roof-Shaped" $Cu_2X_2$ Dimers with Hydroxide, Methoxide, and Azide Bridges

**Bim Graham,[†] Milton T. W. Hearn,[‡] Peter C. Junk,[§] Christopher M. Kepert,[†] Frank E. Mabbs,[||] Boujemaa Moubaraki,[†] Keith S. Murray,[†] and Leone Spiccia*,[†]**

School of Chemistry, PO Box 23, Monash University, Victoria 3800, Australia, Centre for Bioprocess Technology, Department of Biochemistry, Monash University, Clayton, Victoria 3168, Australia, Department of Chemistry, James Cook University of Northern Queensland, Townsville 4811, Australia, and Department of Chemistry, University of Manchester, Manchester M13 9PL, U.K.

*Received August 31, 2000*

Hydroxo- and methoxo-bridged tetranuclear copper(II) complexes of the tetramacrocyclic ligand 1,2,4,5-tetrakis-(1,4,7-triazacyclonon-1-ylmethyl)benzene ($L^{dur}$), have been prepared from $[Cu_4L^{dur}(H_2O)_8](ClO_4)_8 \cdot 9H_2O$ (**1**). Addition of base to an aqueous solution of **1** gave $[Cu_4L^{dur}(\mu_2\text{-}OH)_4](ClO_4)_4$ (**2**). Diffusion of MeOH into a DMF solution of **2** produces $[Cu_4L^{dur}(\mu_2\text{-}OMe)_4](ClO_4)_4 \cdot HClO_4 \cdot 2/3MeOH$ (**3**), a complex which hydrolyzes on exposure to moisture regenerating **2**. The structurally related azido-bridged complex, $[Cu_4L^{dur}(\mu_2\text{-}N_3)_4](PF_6)_4 \cdot 4H_2O \cdot 6CH_3CN$ (**4**), was produced by reaction of $L^{dur}$ with 4 molar equiv of $Cu(OAc)_2 \cdot H_2O$ and $NaN_3$ in the presence of excess $KPF_6$. Compounds **2**−**4** crystallize in the triclinic space group $P\bar{1}$ (No. 2) with $a = 10.248(1)$ Å, $b = 12.130(2)$ Å, $c = 14.353(2)$ Å, $\alpha = 82.23(1)°$, $\beta = 80.79(1)°$, $\gamma = 65.71(1)°$, and $Z = 1$ for **2**, $a = 10.2985(4)$ Å, $b = 12.1182(4)$ Å, $c = 13.9705(3)$ Å, $\alpha = 89.978(2)°$, $\beta = 82.038(2)°$, $\gamma = 65.095(2)°$, and $Z = 1$ for **3**, and $a = 12.059(2)$ Å, $b = 12.554(2)$ Å, $c = 14.051(2)$ Å, $\alpha = 91.85(1)°$, $\beta = 98.22(1)°$, $\gamma = 105.62(1)°$, and $Z = 1$ for **4**. The complexes feature pairs of isolated dibridged copper(II) dimers with "roof-shaped" $Cu_2(\mu_2\text{-}X)_2$ cores ($X = OH^-$, $OMe^-$, $N_3^-$), as indicated by the dihedral angle between the two $CuX_2$ planes (159° for **2**, 161° for **3**, and 153° for **4**). This leads to Cu···Cu distances of 2.940(4) Å for **2**, 2.962(1) Å for **3**, and 3.006(5) Å for **4**. Variable-temperature magnetic susceptibility measurements indicate weak antiferromagnetic coupling ($J = -27$ $cm^{-1}$) for the hydroxo-bridged copper(II) centers in **2** and very strong antiferromagnetic coupling ($J = -269$ $cm^{-1}$) for the methoxo-bridged copper(II) centers in **3**. Pairs of copper(II) centers in **4** display the strongest ferromagnetic interaction ($J = 94$ $cm^{-1}$) reported thus far for bis($\mu_2$-1,1-azido)-bridged dicopper units. Spectral measurements on a neat powdered sample of **4** at 33.9 GHz or 90 Ghz confirm the spin-triplet ground state for the azido-bridged copper(II) pairs.

## Introduction

Binuclear complexes, in which the metal centers are bridged by hydroxo, alkoxo, and azido groups, have featured prominently in magnetochemical studies aimed at developing correlations between molecular structure and magnetic behavior. Hydroxo- and alkoxo-bridged Cu(II) complexes exhibit magnetic behavior ranging from ferromagnetic to antiferromagnetic depending on the geometry of the $Cu_2(OR)_2$ (R = H, alkyl, aryl) bridging units.[1−17] These studies have established that the type and magnitude of the interaction is influenced by the M···M separation, the M−O(bridge) distance, the M−O−M angle ($\theta$), the dihedral angle between the planes formed by the two adjoining CuO units in a $Cu_2O_2$ core, the out-of-plane displacement of substituents on the bridging groups, and the Cu(II) center geometry. Recently, Ruiz et al.[10] have applied density functional (DFT) methods[10] to confirm experimental correlations between the magnetic exchange coupling constant, the M−O−M

* Corresponding author. E-mail: leone.spiccia@sci.monash.edu.au. Fax: +61 3 9905 4597.
[†] School of Chemistry, Monash University.
[‡] Department of Biochemistry, Monash University.
[§] James Cook University of Northern Queensland.
[||] University of Manchester.

(1) Hodgson, D. J. *Prog. Inorg. Chem.* **1975**, *19*, 173.
(2) Cairns, C. J.; Busch, D. H. *Coord. Chem. Rev.* **1986**, *1*, 55.
(3) Hatfield, W. E. In *Magneto-Structural Correlations in Exchange Coupled Systems*; Willett, R. D., Gatteschi, D., Kahn, O., Eds.; NATO-ASI Series; D. Reidel, Dordrecht, The Netherlands, 1984; p 555.
(4) Crawford, V. H.; Richardson, H. W.; Wasson, J. R.; Hodgson, D. J.; Hatfield, W. E. *Inorg. Chem.* **1976**, 15, 2107.
(5) Charlot, M. F.; Jeannin, S.; Jeannin, Y.; Kahn, O.; Lucrece-Aubal, J.; Martin-Frere, J. S. *Inorg. Chem.* **1979**, *18*, 1675.
(6) Charlot, M. F.; Kahn, O.; Jeannin, S.; Jeannin, Y. *Inorg. Chem.* **1980**, *19*, 1410.
(7) Hodgson, D. J. *J. Mol. Catal.* **1984**, *23*, 219.
(8) Haddad, M. S.; Wilson, S. P.; Hodgson, D. J.; Hendrickson, D. N. *J. Am. Chem. Soc.* **1981**, *103*, 384.
(9) Escuer, A.; Vicente, R.; Ribas, J. *Polyhedron* **1992**, *11*, 453.
(10) Ruiz, E.; Alemany, P.; Alvarez, S.; Cano, J. *J. Am. Chem. Soc.* **1997**, *119*, 1297 and references therein.
(11) Castro, I.; Fans, J.; Julve, M.; Lloret, F.; Verdaguer, M.; Kahn, O.; Jeannin, S.; Jeannin, Y.; Vaisserman, J. *J. Chem. Soc., Dalton Trans.* **1990**, 2207.
(12) Merz, L.; Haase, W. *J. Chem. Soc., Dalton Trans.* **1980**, 875.
(13) Willett, R. D.; Breneman, G. L. *Inorg. Chem.* **1983**, *22*, 326.
(14) Drew, M. G. B.; Yates, P. C.; Esho, F. S.; Trocha-Grimshaw, J.; Lavery, A.; McKillop, K. P.; Nelson, S. M.; Nelson J. *J. Chem. Soc., Dalton Trans.* **1988**, 2995.
(15) Fukuhara, C.; Tsuneyoshi, K.; Katsura, K.; Matsumoto, N.; Kida, S.; Mori, M. *Bull. Chem. Soc. Jpn.* **1989**, *62*, 3939.
(16) Drillon, M.; Grand, A.; Rey, P. *Inorg. Chem.* **1990**, *29*, 771.
(17) van Albada, G. A.; Lakin, J. T.; Veldman, N.; Spek, A. L.; Reedijk, J. *Inorg. Chem.* **1995**, *34*, 4910.

10.1021/ic000991h CCC: $20.00 
Published on Web 02/28/2001

angle and the out-of-plane displacement. Ferromagnetic interactions were concluded to be favored by small M−O−M angles (<98°) and large out-of-plane displacements (>50°), in keeping with the experimental data for such compounds.[10]

Azido-bridged complexes of, in particular, copper(II) and nickel(II) have also been the subject of intense investigation aimed at the elucidation of the factors that determine the type of magnetic interaction.[18−30] The azide group in such complexes can adopt two types of bridging modes which generally promote contrasting magnetic behavior (see ref 29 and citations therein). The $\mu_2$-1,1-$N_3$ (end-on) bridging mode promotes ferromagnetic exchange interactions while the $\mu_2$-1,3-$N_3$ (end-to-end) bridging mode generally gives rise to antiferromagnetic exchange coupling between the metal centers. This diversity in magnetic behavior has been exploited in the development of polynuclear assemblies with novel magnetic properties. Examples of such assemblies include materials incorporating both end-on and end-to-end bridging modes.[27,30e] In one interesting complex, the combination of end-on azido, nitrato, and carboxylato bridging has resulted in novel metamagnetic behavior, attributable to the ability of such bridges to mediate contrasting ferromagnetic and antiferromagnetic interactions.[27] Ruiz et al.[29] have also applied DFT methods in the analysis of exchange interactions in end-on bridged Mn(II), Ni(II), and Cu(II) complexes. Electron delocalization and spin polarization were important in determining the strength of ferromagnetic interaction, which varies with the M−N−M angle and M−N distance. In contrast to hydroxo- and alkoxo-bridged complexes, however, the out-of-plane displacement was concluded to have negligible effect on the coupling constant. The M−N−M angle corresponding to the maximum in *J* varied with the metal center, viz., Cu < Ni < Mn. Kahn and co-workers[28] have examined spin density maps for $[Cu_2(t\text{-Bupy})_4(N_3)_2](ClO_4)_2$ obtained from polarized neutron diffraction studies and have also concluded that spin delocalization and spin polarization are important but that DFT calculations tend to overestimate spin delocalization contributions.

We recently described the synthesis of a polynucleating ligand, $L^{dur}$, incorporating four 1,4,7-triazacyclononane (tacn) macrocycles linked by a durene spacer.[31] This ligand was found to be capable of forming bi-, tri-, and tetranuclear complexes, depending on whether each tacn ring coordinated to a different metal center or whether pairs of tacn rings sandwiched a single metal center. The binuclear complex, $[Cu_2L^{dur}](ClO_4)_4\cdot 4H_2O$, and tetranuclear complex, $[Cu_4L^{dur}(H_2O)_8](ClO_4)_8\cdot 9H_2O$ (**1**), were formed exclusively when 2 and 4 equiv of a copper(II) salt were used, respectively.[31] The tetranuclear complex features four magnetically isolated metal centers, with large Cu···Cu separations of 7.04 and 9.54 Å in the solid state. We now report the synthesis of three tetranuclear complexes, $[Cu_4L^{dur}(\mu_2\text{-}OH)_4](ClO_4)_4$ (**2**), $[Cu_4L^{dur}(\mu_2\text{-}OMe)_4](ClO_4)_4\cdot HClO_4\cdot 2/3MeOH$ (**3**), and $[Cu_4L^{dur}(\mu_2\text{-}N_3)_4](PF_6)_4\cdot 4H_2O\cdot 6CH_3CN$ (**4**), in which shorter M···M distances have resulted from the linking of pairs of metal centers by exogenous hydroxo-, methoxo-, and azido-bridging groups, respectively. The X-ray crystal structures of **2**−**4** have been determined and their magnetic properties rationalized in terms of the geometries of the bridged dicopper(II) cores.

## Experimental Section

**Materials and Reagents.** Reagent or analytical grade materials were obtained from commercial suppliers and used without further purification. The $L^{dur}$ ligand and the complex, $[Cu_4L^{dur}(H_2O)_8](ClO_4)_8\cdot 9H_2O$ (**1**), were synthesized as described previously.[31]

**Physical Measurements.** Infrared spectra were recorded on a Perkin-Elmer 1600 FTIR spectrophotometer, as KBr pellets or Nujol mulls, and electronic spectra on a Cary 5 spectrophotometer. Electron microprobe analyses were made with a JEOL JSM-1 scanning electron microscope through an NEC X-ray detector and pulse-processing system connected to a Packard multichannel analyzer. ESR spectra were recorded in Manchester University using a Bruker ESP-300E-12/15 Z instrument operating at microwave frequencies of 33.9 or 90 GHz. Typical instrument settings at 33.9 GHz were the following: receiver gain, 500; modulation frequency, 100 kHz; modulation amplitude, 10 G; microwave power, 0.915 mW. Temperatures were controlled at 10, 15, 20, 40, 60, 80, 100, 120, and 290 K for Q-band measurements and at 6, 10, 15, 25, and 50 K for 90 GHz measurements. Variable-temperature magnetic susceptibilities were measured using a Quantum Design MPMS5 SQUID magnetometer operating in an applied field of 1 T. The powdered samples were contained in calibrated gelatine capsules held in the center of a straw, the latter being attached to the end of the sample rod. The temperature and field were checked against a standard Pd sample and $CuSO_4\cdot 5H_2O$. Fitting of the magnetic data employed a nonlinear least-squares program called POLYMER written at Monash University by Dr. E. N. Bakshi and Mr. K. J. Berry.

**Caution!** Although no problems were encountered in this work, transition metal perchlorates are potentially explosive. They should be prepared in small quantities and handled with care.

**Preparations. (a) $[Cu_4L^{dur}(\mu_2\text{-}OH)_4](ClO_4)_4$ (2).** A solution of $[Cu_4L^{dur}(H_2O)_8](ClO_4)_8\cdot 9H_2O$ (**1**) (0.15 g, 0.075 mmol) in $H_2O$ (10 mL) was heated on a steam bath and the pH adjusted to 9.5 with 2 M NaOH solution. $NaClO_4$ (1.00 g, 8.17 mmol) was then added and the solution left to stand. A fine blue precipitate of **2** formed overnight, which was collected by filtration, washed with MeOH, and air-dried. Yield: 0.070 g, 68%. Anal. Calcd for $[Cu_4(C_{34}H_{66}N_{12})(\mu_2\text{-}OH)_4](ClO_4)_4$: C, 30.0; H, 5.2; N, 12.3. Found: C, 30.0; H, 5.5; N, 12.2. Electron microprobe: Cu and Cl uniformly present. UV−visible spectrum ($H_2O$): $\lambda_{max}$ ($\epsilon_{max}$) = 612 (316), ~880 sh. Selected IR bands (KBr, $cm^{-1}$): 3445 vs br, 3300 s, 2936 m, 1638 m br, 1495 m, 1455 m, 1363 m, 1091 vs br, 626 s. Crystals suitable for crystallography were grown by diffusion of MeOH into a DMF solution of **2**. This initially results in formation of **3** (see below), which is slowly converted back into **2** on exposure to moisture.


(18) Cormarmond, J.; Pluméré, P.; Lehn, J. M.; Agnus, Y.; Louis, R.; Weiss, R.; Kahn, O.; Morgenstern-Baderau, I. *J. Am. Chem. Soc.* **1982**, *104*, 6330.

(19) Kahn, O.; Sikorav, S.; Gouteron, J.; Jeannin, S.; Jeannin, V. *Inorg. Chem.* **1983**, *22*, 2877.

(20) Sikorav, S.; Bkouche-Waksman, I.; Kahn, O. *Inorg. Chem.* **1984**, *23*, 490.

(21) Chaudhuri, P.; Oder, K.; Wieghardt, K.; Nuber, B.; Weiss, J. *Inorg. Chem.* **1986**, *25*, 2818.

(22) Charlot, M.-F.; Kahn, O.; Chaillet, M.; Larrieu, C. *J. Am. Chem. Soc.* **1986**, *108*, 2574.

(23) Tandon, S. S.; Thompson, L. K.; Manuel, M. E.; Bridson, J. N. *Inorg. Chem.* **1994**, *33*, 5555.

(24) Tuczek, F.; Bensch, W. *Inorg. Chem.* **1995**, *34*, 1482.

(25) Thompson, L. K.; Tandon, S. S.; Manuel, M. E. *Inorg. Chem.* **1995**, *34*, 2356.

(26) Von Seggern, I.; Tuczek, F.; Bensch, W. *Inorg. Chem.* **1995**, *34*, 5530.

(27) Thompson, L. K.; Tandon, S. S.; Lloret, F.; Cano, J.; Julve, M. *Inorg. Chem.* **1997**, *36*, 3301.

(28) Aebersold, M. A.; Gillon, B.; Plantevin, O.; Pardi, L.; Kahn, O.; Bergerat, P.; Vv Seggern, I.; Tuczek, F.; Öhrström, L.; Grand, A.; Lelièvre-Berne, E. *J. Am. Chem. Soc.* **1998**, *120*, 5238.

(29) Ruiz, E.; Cano, J.; Alvarez, S.; Alemany, P. *J. Am. Chem. Soc.* **1998**, *120*, 11122.

(30) (a) Vicente, R.; Escuer, A.; Ribas, J.; Solans, X. *Inorg. Chem.* **1992**, *31*, 1726. (b) Escuer, A.; Vicente, R.; Ribas, J.; El Fallah, M. S.; Solans, X.; Font-Bardie, M. *Inorg. Chem.* **1993**, *32*, 3727. (c) Vicente, R.; Escuer, A.; Ribas, J.; El Fallah, M. S.; Solans, S.; Font-Bardie, M. *Inorg. Chem.* **1993**, *32*, 1920. (d) Ribas, J.; Monfort, M.; Diaz, C.; Bastos, C.; Solans, X. *Inorg. Chem.* **1993**, *32*, 3557. (e) Ribas, J.; Monfort, M.; Solans, X.; Drillon, M. *Inorg. Chem.* **1994**, *33*, 742. (f) Escuer, A.; Vicente, R.; Ribas, J.; El Fallah, M. S.; Solans, X.; Font-Bardie, M. *Inorg. Chem.* **1994**, *33*, 1842. (g) McLachlan, G. A.; Fallon, G. D.; Martin, R. L.; Moubaraki, B.; Murray, K. S.; Spiccia, L. *Inorg. Chem.* **1994**, *33*, 4663.

(31) Graham, B.; Grannas, M. J.; Hearn, M. T. W.; Kepert, C. M.; Spiccia, L.; Skelton, B. W.; White, A. H. *Inorg. Chem.* **2000**, 39, 1092.

**Table 1.** Crystallographic Data for $[Cu_4L^{dur}(\mu_2\text{-}OH)_4](ClO_4)_4$ (**2**), $[Cu_4L^{dur}(\mu_2\text{-}OMe)_4](ClO_4)_4{\cdot}HClO_4{\cdot}2/3MeOH$ (**3**), and $[Cu_4L^{dur}(\mu_2\text{-}N_3)_4](PF_6)_4{\cdot}4H_2O{\cdot}6CH_3CN$ (**4**)

| | | | |
|---|---|---|---|
| chem formula | $C_{34}H_{70}Cu_4Cl_4N_{12}O_{20}$ | $C_{38.66}H_{73.66}Cu_4Cl_5N_{12}O_{24.66}$ | $Cu_{46}H_{92}Cu_4F_{24}N_{30}O_4P_4$ |
| fw | 1363.0 | 1532.7 | 1963.48 |
| space group | $P\bar{1}$ | $P\bar{1}$ | $P\bar{1}$ |
| *a*, Å | 10.248(1) | 10.2985(4) | 12.059(2) |
| *b*, Å | 12.130(2) | 12.1182(4) | 12.554(2) |
| *c*, Å | 14.353(2) | 13.9705(3) | 14.051(2) |
| α, deg | 82.23(1) | 89.978(2) | 91.85(1) |
| *β*, deg | 80.79(1) | 82.038(2) | 98.22(1) |
| *γ*, deg | 65.71(1) | 65.095(2) | 105.62(1) |
| *V*, Å$^3$ | 1600.6(5) | 1562.87(9) | 2022.1(6) |
| *Z* | 1 | 1 | 1 |
| *T*, K | 296 | 123 | 296 |
| *λ*, Å | 0.710 73 | 0.710 69 | 0.710 73 |
| $D_c$, g cm$^{-3}$ | 1.414 | 1.628 | 1.591 |
| $\mu$(Mo Kα), cm$^{-1}$ | 15.5 | 16.4 (no correction) | 12.3 |
| $R^a$ ($R_w{}^b$) | 0.078 (0.074) | 0.082 (0.097)$^c$ | 0.068 (0.069) |

$^a$ $R = \Sigma(|F_o| - |F_c|)/\Sigma|F_o|$. $^b$ $R_w = [\Sigma w(|F_o| - |F_c|)^2/\Sigma wF_o^2]^{1/2}$. $^c$ Unit weighting scheme used.

**(b)$[Cu_4L^{dur}(\mu_2\text{-}OMe)_4](ClO_4)_4{\cdot}2MeOH$ (3).** Layering of a DMF solution of **2** with MeOH resulted in deposition of crystals of **3**. Anal. Calcd for $[Cu_4(C_{34}H_{66}N_{12})(\mu_2\text{-}OMe)_4](ClO_4)_4{\cdot}2MeOH$: C, 32.4; H, 5.8; N, 11.3. Found: C, 32.6; H, 6.0; N, 11.4. Electron microprobe: Cu and Cl uniformly present. Selected IR bands (KBr, cm$^{-1}$): 3424 vs br, 3312 s, 2929 m, 1671 m br, 1492 m, 1456 m, 1361 m, 1092 vs br, 625 s. A crystal suitable for X-ray crystallography was of composition $[Cu_4L^{dur}(\mu_2\text{-}OMe)_4](ClO_4)_4{\cdot}HClO_4{\cdot}2/3MeOH$ (**3**).

**(c) $[Cu_4L^{dur}(\mu_2\text{-}N_3)_4](PF_6)_4{\cdot}4H_2O{\cdot}6CH_3CN$ (4).** $Cu(OAc)_2{\cdot}H_2O$ (0.060 g, 0.30 mmol) and $L^{dur}$ (0.048 g, 0.075 mmol) were dissolved in $H_2O$ (50 mL) to afford a dark blue solution. Addition of $NaN_3$ (0.020 g, 0.30 mmol) gave a dark green solution and a small amount of a grey precipitate. The mixture was filtered and $KPF_6$ (0.15 g, 0.81 mmol) added to the filtrate, resulting in the immediate formation of a green precipitate which was filtered out and dissolved in $CH_3CN$ (10 mL). Slow evaporation deposited dark green crystals of the tetrahydrate hexakis(acetonitrile) adduct suitable for X-ray crystallography. These were collected by vacuum filtration, washed with MeOH, and air-dried. During the drying process the crystals became "frosty", indicating loss of solvent from the crystal lattice. Microanalytical data collected on these crystals corresponded to the tetrahydrate. Yield: 0.067 g, 52%. Anal. Calcd for $[Cu_4(C_{34}H_{66}N_{12})(\mu_2\text{-}N_3)_4](PF_6)_4{\cdot}4H_2O$: C, 23.8; H, 4.3; N, 19.6. Found: C, 24.0; H, 4.2; N, 19.2. Electron microprobe: Cu and Cl uniformly present. UV−visible spectrum ($CH_3CN$): $\lambda_{max}$ ($\epsilon_{max}$) = 355 (8640), 376 (8380), 618 (610). Selected IR bands (KBr, cm$^{-1}$): 3417 vs br, 3220 m, 2945 w, 2107 m, 2067 vs, 1638 s, 1618 s, 1492 w, 1458 m, 1361 w, 1290 m, 846 vs, 558 m.

**X-ray Crystallography.** Intensity data for a dark blue block of **2** (0.48 × 0.46 × 0.40 mm) and a dark green-blue crystal of **4** (0.14 × 0.20 × 0.07 mm) were measured at 296 K on an Enraf-Nonius CAD-4 diffractometer using the $2\theta/\theta$ scan mode to a maximum $2\theta$ value of 50.0°. The crystal of **2** decomposed ca. 50% during the data collection. "Observed" reflections were used in the full-matrix least-squares refinements after Gaussian absorption correction. All non-hydrogen atoms were refined with anisotropic thermal parameters. Hydrogens were included in calculated positions but not refined. A statistical weights derivative of $\sigma^2(I) = \sigma^2(I_{diff}) + 0.0004\sigma^4(I_{diff})$ was used. Neutral atom scattering factors were used and computation performed using the Xtal 3.4 program system.[32]

For **3**, intensity data for a cubic section of a dark blue rectangular prismatic crystal (0.10 × 0.10 × 0.10 mm) were collected at 123K on a Eraf-Nonius Kappa CCD diffractometer operating in the $\omega$ scan mode to a maximum $2\theta$ value of 55°. Structure solution was effected by analysis of "observed" reflections with direct methods. Anisotropic thermal parameters were refined for non-hydrogen atoms in the complex, in the full-matrix least-squares refinement of 397 variables. Some atoms in the perchlorate counterions were refined using isotropic thermal parameters. Hydrogens were included at idealized geometric positions. Disorder in one perchlorate was modeled as the partial occupancy of two sites. Difference map residues were modeled in terms of methanol solvent. Calculations were performed using teXsan[33] employing neutral atom complex scattering factors. Note that the data were best fitted with unit weights. Three different batches of crystals were examined, but in each case statistical weighting gave a much poorer fit than unit weights indicating that this is a feature intrinsic to crystals of **3**. Despite this, the connectivity and structural features of the complex cation are sufficiently well defined to allow rationalization of the magnetic data.

Crystal parameters and details of data collection and refinement for **2**−**4** are given in Table 1. Selected bond distances and angles are given in Tables 2−4, and ORTEP views of the complex cations the are presented in Figures 2−4.

**Table 2.** Selected Bond Distances (Å) and Angles (deg) for $[Cu_4L^{dur}(\mu_2\text{-}OH)_4](ClO_4)_4$ (**2**)

| | | | |
|---|---|---|---|
| Cu(1)−O(1) | 1.961(8) | Cu(1)−O(2) | 1.975(8) |
| Cu(1)−N(1b) | 2.024(8) | Cu(1)−N(2b) | 2.346(9) |
| Cu(1)−N(3b) | 2.032(9) | Cu(2)−O(1) | 1.936(7) |
| Cu(2)−O(2) | 1.989(9) | Cu(2)−N(1a) | 2.04(1) |
| Cu(2)−N(2a) | 2.354(9) | Cu(2)−N(3a) | 1.979(9) |
| O(1)−Cu(1)−O(2) | 80.8(4) | O(1)−Cu(1)−N(1b) | 95.9(4) |
| O(1)−Cu(1)−N(2b) | 110.0(4) | O(1)−Cu(1)−N(3b) | 168.8(3) |
| O(2)−Cu(1)−N(1b) | 165.6(3) | O(2)−Cu(1)−N(2b) | 111.6(4) |
| O(2)−Cu(1)−N(3b) | 96.4(4) | N(1b)−Cu(1)−N(2b) | 82.7(4) |
| N(1b)−Cu(1)−N(3b) | 84.1(4) | N(2b)-Cu(1)−N(3b) | 81.2(4) |
| O(1)−Cu(2)−O(2) | 81.0(4) | O(1)−Cu(2)−N(1a) | 96.3(4) |
| O(1)−Cu(2)−N(2a) | 108.5(4) | O(1)−Cu(2)−N(3a) | 170.0(3) |
| O(2)−Cu(2)−N(1a) | 165.9(3) | O(2)−Cu(2)−N(2a) | 112.8(4) |
| O(2)−Cu(2)−N(3a) | 96.4(4) | N(1a)−Cu(2)−N(2a) | 81.3(4) |
| N(1a)−Cu(2)−N(3a) | 83.8(4) | N(2a)−Cu(2)−N(3a) | 81.4(4) |
| Cu(1)−O(1)−Cu(2) | 97.9(4) | Cu(1)−O(2)−Cu(2) | 95.7(4) |

## Results and Discussion

**Synthesis and Characterization of Complexes.** Adjustment of the pH of an aqueous solution of $[Cu_4L^{dur}(H_2O)_8](ClO_4)_8{\cdot}9H_2O$ (**1**) to ca. 9.5 results in hydroxo-bridge formation between pairs of meta-oriented Cu(II)−tacn units and immediate precipitation of the perchlorate salt, $[Cu_4L^{dur}(\mu_2\text{-}OH)_4](ClO_4)_4$ (**2**). Diffusion of methanol into a DMF solution of **2** gave a compound with methoxo groups bridging pairs of Cu(II) centers (see crystal structure) and corresponding to the $[Cu_4L^{dur}(\mu_2\text{-}OMe)_4](ClO_4)_4{\cdot}2MeOH$ (**3**) (the crystal structure of the methanolate perchloric acid adduct is described below). When **3** is left in air, slow hydrolysis of the methoxo bridges occurred regenerating **2** in a crystalline form suitable for X-ray crystal-

(32) Hall, S. R.; King, G. S. P.; Stewart, J. M. *The Xtal 3.4 User's Manual*; University of Western Australia, Lamb Print: Perth, Australia, 1994.

(33) *teXan: Crystal Structure Analysis Package*; Molecular Structure Corp.: Houston, TX, 1992.

**Table 3.** Selected Bond Distances (Å) and Angles (deg) for $[Cu_4L^{dur}(\mu_2\text{-}OMe)_4](ClO_4)_4\cdot HClO_4\cdot 2/3MeOH$ (**3**)

| | | | |
|---|---|---|---|
| Cu(1)−O(1) | 1.922(6) | Cu(1)−O(2) | 1.954(6) |
| Cu(1)−N(1a) | 2.028(7) | Cu(1)−N(2a) | 2.353(7) |
| Cu(1)−N(3a) | 2.032(7) | Cu(2)−O(1) | 1.938(6) |
| Cu(2)−O(2) | 1.949(6) | Cu(2)−N(1b) | 2.033(7) |
| Cu(2)−N(2b) | 2.365(7) | Cu(2)−N(3b) | 2.023(7) |
| O(1)−Cu(1)−O(2) | 78.7(2) | O(1)−Cu(1)−N(1a) | 96.2(3) |
| O(1)−Cu(1)−N(2a) | 111.8(2) | O(1)−Cu(1)−N(3a) | 166.5(3) |
| O(2)−Cu(1)−N(1a) | 166.2(3) | O(2)−Cu(1)−N(2a) | 111.3(2) |
| O(2)−Cu(1)−N(3a) | 97.5(3) | N(1a)−Cu(1)−N(2a) | 82.4(3) |
| N(1a)-Cu(1)−N(3a) | 84.4(3) | N(2a)−Cu(1)−N(3a) | 81.7(3) |
| O(1)−Cu(2)−O(2) | 78.5(2) | O(1)−Cu(2)−N(1b) | 96.4(3) |
| O(1)−Cu(2)−N(2b) | 110.0(2) | O(1)−Cu(2)−N(3b) | 168.4(3) |
| O(2)−Cu(2)−N(1b) | 165.1(3) | O(2)−Cu(2)−N(2b) | 113.2(2) |
| O(2)−Cu(2)−N(3b) | 97.5(3) | N(1b)−Cu(2)−N(2b) | 81.7(2) |
| N(1b)−Cu(2)−N(3b) | 84.8(3) | N(2b)−Cu(2)−N(3b) | 81.6(3) |
| Cu(1)−O(1)−Cu(2) | 100.2(3) | Cu(1)−O(2)−Cu(2) | 98.7(3) |

**Table 4.** Selected Bond Distances (Å) and Angles (deg) for $[Cu_4L^{dur}(\mu_2\text{-}N_3)_4](PF_6)_4\cdot 4H_2O\cdot 6CH_3CN$ (**4**)

| | | | |
|---|---|---|---|
| Cu(1)−N(1) | 2.012(9) | Cu(1)−N(4) | 1.993(9) |
| Cu(1)−N(1a) | 1.996(9) | Cu(1)−N(2a) | 2.295(9) |
| Cu(1)−N(3a) | 2.016(9) | Cu(2)−N(1) | 1.970(9) |
| Cu(2)−N(4) | 2.03(1) | Cu(2)−N(1b) | 2.02(1) |
| Cu(2)−N(2b) | 2.291(9) | Cu(2)−N(3b) | 2.00(1) |
| N(1)−N(2) | 1.19(1) | N(2)−N(3) | 1.13(1) |
| N(4)−N(5) | 1.20(1) | N(5)−N(6) | 1.14(2) |
| N(1)−Cu(1)−N(4) | 80.0(4) | N(1)−Cu(1)−N(1a) | 96.4(4) |
| N(1)−Cu(1)−N(2a) | 107.2(4) | N(1)−Cu(1)−N(3a) | 168.7(3) |
| N(4)−Cu(1)−N(1a) | 164.5(4) | N(4)−Cu(1)−N(2a) | 111.6(4) |
| N(4)−Cu(1)−N(3a) | 96.0(4) | N(1a)−Cu(1)−N(2a) | 82.4(4) |
| N(1a)−Cu(1)−N(3a) | 84.6(4) | N(2a)−Cu(1)−N(3a) | 83.9(4) |
| N(1)−Cu(2)−N(4) | 80.0(4) | N(1)−Cu(2)−N(1b) | 94.7(4) |
| N(1)−Cu(2)−N(2b) | 106.0(4) | N(1)−Cu(2)−N(3b) | 168.0(3) |
| N(4)−Cu(2)−N(1b) | 163.7(3) | N(4)−Cu(2)−N(2b) | 111.6(4) |
| N(4)−Cu(2)−N(3b) | 96.5(4) | N(1b)−Cu(2)−N(2b) | 83.7(4) |
| N(1b)−Cu(2)−N(3b) | 85.5(4) | N(2b)−Cu(2)−N(3b) | 81.9(4) |
| Cu(1)−N(1)−Cu(2) | 98.1(4) | Cu(1)−N(4)−Cu(2) | 96.6(4) |

lography. The preservation of crystal quality during this transformation may be facilitated by the relatively small differences in unit cell parameters for the two compounds (Table 1). A structurally related azido-bridged complex, $[Cu_4L^{dur}(\mu_2\text{-}N_3)_4](PF_6)_4\cdot 4H_2O\cdot 6CH_3CN$ (**4**), was produced by reaction of $L^{dur}$ with 4 molar equiv of both $Cu(OAc)_2\cdot H_2O$ and $NaN_3$ in the presence of excess $KPF_6$. Schematic representations of the complexes are shown in Figure 1.

Microanalytical and electron microprobe data supported the proposed formulations for **2** and **3**. In the case of **4**, the sample used in analytical and spectroscopic characterization was the tetrahydrate adduct, while a tetrahydrate hexakis(acetonitrile) adduct was used in the X-ray structural analysis. Distinctive bands at 2107 and 2067 $cm^{-1}$, assigned to $\nu_{asym}(N_3^-)$, and 1290 $cm^{-1}$, assigned to $\nu_{sym}(N_3^-)$, in the IR spectrum of **4** confirmed the presence of bridging azido groups. The asymmetric nature of the $[Cu_2(\mu_2\text{-}N_3)_2]^{2+}$ cores within **4** (see crystal structure) can account for the appearance of two $\nu_{asym}(N_3^-)$ bands. The position of the bands further indicates that the azido groups have adopted a $\mu$-1,1 end-on rather than the alternative $\mu$-1,3 end-to-end coordination mode, a feature also confirmed by the crystal structure.

The UV−vis spectrum of **2** shows a broad d−d band centered at 612 nm with a shoulder at ca. 880 nm, in agreement with a $(d_{x^2-y^2})^1$ electronic ground-state of a Cu(II) ion in a SP geometry, for which $d_{z^2} \rightarrow d_{x^2-y^2}$ and $d_{xz}$, $d_{yz} \rightarrow d_{x^2-y^2}$ transitions are expected.[34] The substantial blue-shift in these bands relative to the corresponding bands observed at 650 and 1052 nm for the aquo complex, **1**, indicates an overall increase in the ligand field strength surrounding each Cu(II) center. Compound **4** exhibits a d−d absorption at 618 nm, together with two intense overlapping bands at 355 and 376 nm, assigned to azide → $Cu^{II}$ charge-transfer transitions.[26]

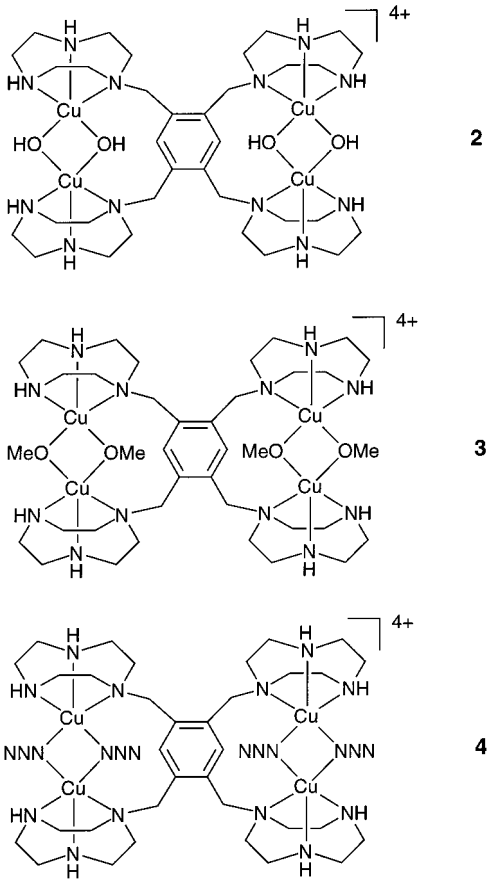


**Figure 1.** Hydroxo- and azido-bridged copper(II) complexes of $L^{dur}$.

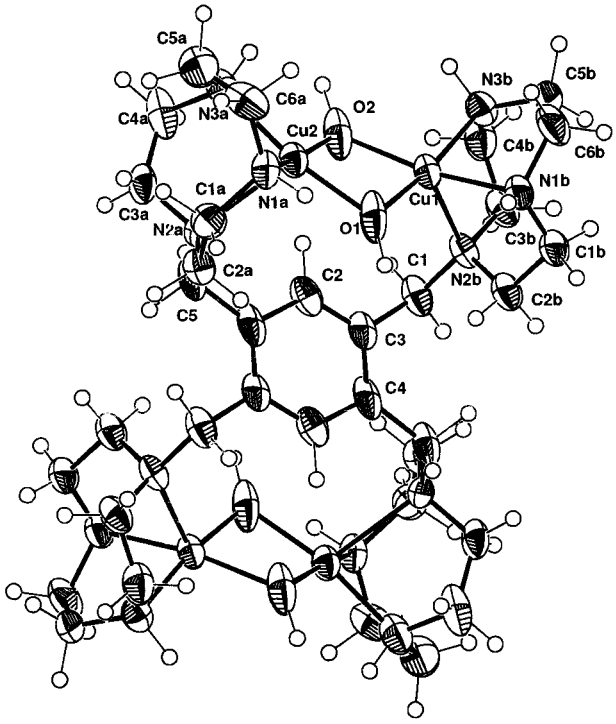


**Figure 2.** ORTEP plot of the molecular cation in **2** with the atomic labeling scheme. Thermal ellipsoids are drawn at the 50% probability level.

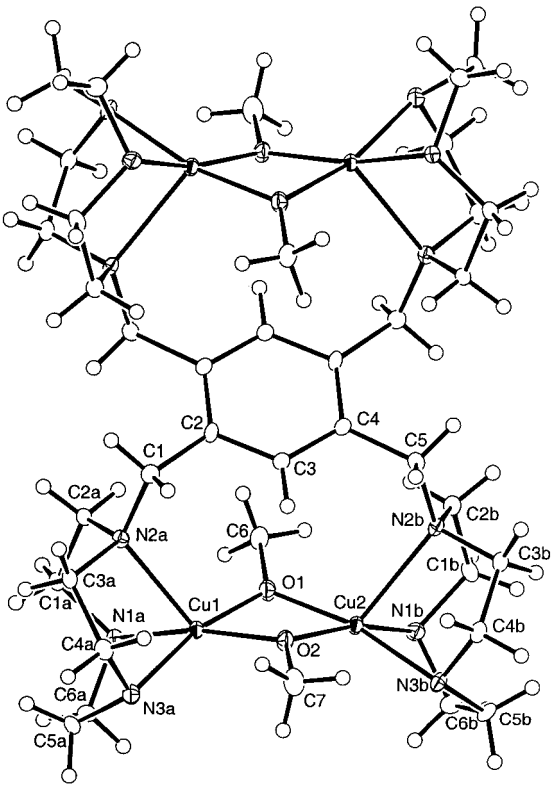


**Figure 3.** ORTEP plot of the molecular cation in **3** with the atomic labeling scheme. Thermal ellipsoids are drawn at the 25% probability level.

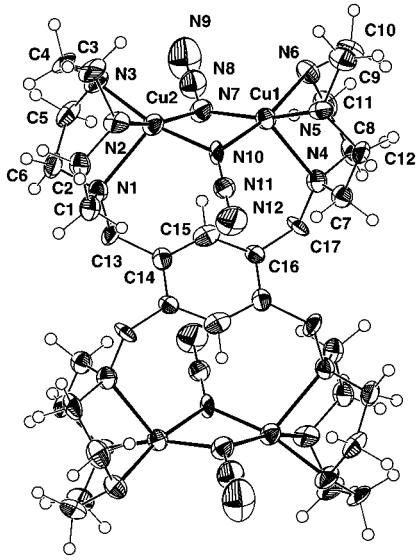


**Figure 4.** ORTEP plot of the molecular cation in **4** with the atomic labeling scheme. Thermal ellipsoids are drawn at the 50% probability level.

**Crystal Structures.** To confirm the "pair-of-dimers" structures proposed for **2**−**4**, the single-crystal X-ray structures were determined. The crystals contain the tetranuclear cations, $[Cu_4L^{dur}(\mu_2\text{-}OH)_4]^{4+}$ (**2**), $[Cu_4L^{dur}(\mu_2\text{-}OMe)_4]^{4+}$ (**3**), and $[Cu_4L^{dur}(\mu_2\text{-}N_3)_4]^{4+}$ (**4**), which feature pairs of "roof-shaped" $Cu_2X_2$ dimeric units.

The cations in **2** and **3** consist of two symmetry-related di-$\mu_2$-hydroxo- and di-$\mu_2$-methoxo-bridged copper(II) dimeric units which lie on opposite sides of the plane of the central aromatic ring of the $L^{dur}$ ligand (Figures 2 and 3). The two $Cu_2O_2$ units are capped by pairs of tacn rings. Relative to each other, these tacn rings are attached at meta positions on the aromatic ring of the durene spacer group. The copper(II) centers exhibit distorted square pyramidal (SP) coordination polyhedra, with the tertiary bridgehead nitrogens occupying the axial positions [Cu−N(axial) ∼ 2.35 Å]. Two secondary amine nitrogens from the tacn rings and oxygen atoms from either the hydroxo or methoxo groups form the basal plane. Estimates of the degree of distortion from ideal SP geometry obtained by applying $\tau$ the geometric parameter developed by Addison et al.[35] indicate geometries close to regular SP [for **2** $\tau = 5\%$ for Cu(1) and 7% for Cu(2) while for **3** $\tau = 0\%$ for Cu(1) and 6% for Cu(2)]. The N−Cu−N angles, however, are characteristically reduced from 90° (81−85°) due to the facial coordination mode of the tacn macrocycle, which involves the formation of three fused five-membered chelate rings, and the Cu−O−Cu angles are typical of those observed in similar complexes (see Table 5).

In contrast to the planar $Cu_2(\mu_2\text{-}OH)_2$ geometry found in $[Cu_2(Me_3tacn)_2(\mu_2\text{-}OH)_2](ClO_4)_2$ and other "unsupported" hydroxo[2] and alkoxo[13−16] bridged binuclear complexes, the $Cu_2O_2$ bridging units in **2** and **3** adopt bent, or "roof-shaped", conformations. This distortion is evident from the dihedral angle ($\delta$) between the Cu(1)/O(1)/O(2) and Cu(2)/O(1)/O(2) planes of 159° in **2** and 161° in **3**. In the case of **2**, the Cu···Cu separation (2.939(9) Å) is slightly shorter than in the related but "unsupported" $[Cu_2(Me_3tacn)_2(\mu_2\text{-}OH)_2](ClO_4)_2$ (2.971(1) Å) complex.[36] Similar trends are evident for the alkoxo-bridged complexes; viz., the Cu···Cu distance of 2.962(1) Å in **3** is shorter than those generally found in complexes with planar $Cu_2O_2$ cores.[13−17] "Roof-shaped" $Cu_2O_2$ cores have been observed in $[Cu_2(C_6H_{11}NH_2)_4(\mu_2\text{-}OH)_2](ClO_4)_2$[5] and $[Cu_2(CH_3NH_2)_4(\mu_2\text{-}OH)_2](SO_4)\cdot H_2O$,[6] which show dihedral angles of 148 and 133° and Cu···Cu distances of 2.934(8) and 2.782(5) Å, respectively. Thus, the bending of the $Cu_2(\mu_2\text{-}OH)_2$ cores in **2** is not necessarily due to constraints imposed by the durene tether. Indeed, although the related complex $[Cu_2L^{mx}(\mu_2\text{-}OH)_2](BPh_4)_2$ [$L^{mx}$ = 1,3-bis(1,4,7-triazacyclonon-1-ylmethyl)benzene] has a similar backbone, the $Cu_2(\mu_2\text{-}OH)_2$ core is only very slightly bent, $\delta = 174°$.[37] The Cu···Cu distances across the durene spacer and the internuclear distances to Cu centers on neighboring molecules are greater than 8 Å, as was the case for nonbridged Cu(II) and Ni(II) complexes of the same ligand.[31]

A further notable feature of **2**, **3,** and $[Cu_2L^{mx}(\mu_2\text{-}OH)_2](BPh_4)_2$ is that tethering of the tacn rings enforces a cisoid arrangement of the two edge-sharing $CuN_3O_2$ polyhedra, with the two apical bridgehead nitrogens lying on the same side of the $Cu_2O_2$ unit. In contrast, the apical nitrogens in the centrosymmetric copper(II) dimer incorporating $Me_3$tacn as the capping ligand adopt a transoid conformation with respect to the $Cu_2O_2$ plane.[36]

The cation in **4** is also centrosymmetric about the midpoint of the aromatic ring of the $L^{dur}$ ligand (Figure 4). Both pairs of meta-oriented $Cu^{2+}$-tacn moieties are bridged by two azide ligands binding in a $\mu$-1,1 end-on fashion. The copper(II) geometry is once again dictated by the tacn macrocycles and is very close to SP [$\tau = 7\%$ for Cu(1) and Cu(2)]. The bridgehead nitrogens occupy the axial positions [Cu−N = 2.29 Å], with

(34) Hathaway, B. J. In *Comprehensive Coordination Chemistry*; Wilkinson, G., Gillard, R. D., McCleverty, J. A., Eds.; Pergamon Press: Oxford, England, 1987; p 533.

(35) Addison, A. W.; Rao, T. N.; Reedijk, J.; van Rijn, J.; Verschoor, G. C. *J. Chem. Soc., Dalton Trans.* **1984**, 1349.

(36) Chaudhuri, P.; Ventur, D.; Wieghardt, K.; Peters, E.-M.; Peters, K.; Simon, A. *Angew. Chem., Int. Ed. Engl.* **1985**, *24*, 57.

(37) Farrugia, L. J.; Lovatt, P. A.; Peacock, R. P. *J. Chem. Soc., Dalton Trans.* **1997**, 911.

**Table 5.** Structural and Magnetic Properties of **2**−**4** and Selected Di-$\mu_2$-Hydroxo-, Di-$\mu_2$-Alkoxo-, and Di-$\mu_2$-1,1-Azido-Bridged Copper(II) Complexes

| complex | Cu−X−Cu (deg) | Cu···Cu (Å) | Cu−X (Å) | $\delta^a$ (deg) | $J$ (cm$^{-1}$) |
|---|---|---|---|---|---|
| | | Hydroxo-Bridged Complexes | | | |
| **2** | 97.9(4) | 2.939(9) | 1.961(8) | 159 | −27 |
| | 95.7(4) | | 1.975(8) | | |
| $[Cu_2(Me_3tacn)_2(\mu_2\text{-}OH)_2](ClO_4)_2$[b] | 100.1(2) | 2.971(1) | 1.939(4) | 180 | −45 |
| $[Cu_2(C_6H_{11}NH_2)_4(\mu_2\text{-}OH)_2](ClO_4)_2$[c] | 96.6(2) | 2.934(8) | 1.960(5) | 148 | −128 |
| | 99.7(2) | | 1.923(5) | | |
| $[Cu_2(CH_3NH_2)_4(\mu_2\text{-}OH)_2](SO_4)\cdot H_2O$[d] | 91.7(7) | 2.782(5) | 1.99(1) | 133 | −4 |
| | 88.6(7) | | 1.94(1) | | |
| $[Cu_2L^{mx}(\mu_2\text{-}OH)_2](BPh_4)_2$[e] | 99.6(1) | 2.9464(5) | 1.931(2) | 173 | −80 |
| | | Alkoxo-Bridged Complexes | | | |
| **3** | 100.2(3) | 2.962(1) | 1.922(6) | 161 | −269 |
| | 98.7(3) | | 1.954(6) | | |
| $[Cu_2(OPPA)_2(\mu_2\text{-}OEt)_2]$[f] | 103.0(2) | 2.974(1) | 1.899(3) | 180 | −269 |
| $[Cu_2(py)_2(\mu_2\text{-}OMe)_2Cl_2]$[g] | 103.2(1) | 3.037(2) | 1.940(6) | 180 | −355 |
| $[Cu_2(Et_2N(CH_2)_2(CH_2)_3O)_2](ClO_4)_2$[h] | 99.4 | 2.953 | 1.935 | 165 | −265 |
| $[Cu_2(Me_2N(CH_2)_3(CH_2)_3O)_2](ClO_4)_2$[h] | 98.4 | 2.939 | 1.941 | 158 | −230 |
| | | $\mu$-1,1-Azido-Bridged Complexes | | | |
| **4** | 98.1(4) | 3.006(5) | 2.012(9) | 153 | 94 |
| | 96.6(4) | | 1.996(9) | | |
| $[Cu_2(OBISDIEN)(\mu_2\text{-}N_3)_2(N_3)_2]\cdot H_2O$[i] | 105.5(1) | 3.162(1) | 1.990(2) | 178 | 35 |
| | 101.6(1) | | 2.043(2) | | |
| $[Cu_2(DMPTD)(\mu_2\text{-}N_3)_2(N_3)_2]$[j] | 98.3(4) | 3.076(2) | 1.995(9) | 160 | 85 |
| | 101.9(4) | | 2.043(9) | | |
| $[Cu_2(t\text{-}Bupy)_4(\mu_2\text{-}N_3)_2](ClO_4)_2$[k] | 100.5(6) | 3.042(3) | 1.99(1) | 180 | 53 |
| $[Cu_2(tbz)_2(\mu_2\text{-}N_3)_2(N_3)_2]\cdot 2CH_3OH$[l] | 104.7(2) | 3.2422(9) | 2.059(4) | 180 | 12 |
| | | | | 2.037(4) | |

[a] Dihedral angle between two $CuO_2$ planes. [b] Reference 36, $Me_3tacn$ = 1,4,7-trimethyl-1,4,7-triazacyclononane. [c] Reference 5. [d] Reference 6. [e] Reference 37, $L^{mx}$ = 1,3-bis(1,4,7-triazacyclonon-1-ylmethyl)benzene). [f] Reference 16, OPPA = (1-oxy-2,2,6,6-tetramethylpiperidin-4-yl)pivaloylacetato. [g] Reference 13. [h] Reference 39. [i] Reference 18, OBISDIEN = 1,13-dioxa-4,7,10,16,19,23-hexaazacyclotetracosane. [j] Reference 24, DMPTD = 2,5-bis((pyridylmethyl)thio)thiadiazole. [k] Reference 29, *t*-Bupy = 4-*tert*-butylpyridine. [l] Reference 17, tbz = bis(2-benzimidazolyl)propane.

the secondary nitrogens of the tacn rings and the azido nitrogens lying in the basal plane [Cu−N = 1.970(9) −2.03(1) Å]. The Cu−N(azido) bond lengths match those observed in related compounds.[18−21,24,25]

The preference for a $\mu$-1,1-azido bridging mode in **4**, rather than the end-to-end disposition favored in the "unsupported" dimer, $[Cu_2(Me_3tacn)_2(\mu_2\text{-}N_3)_2](ClO_4)_2$, derives from the linkage of the four tacn units through a durene unit.[21] Similar $Cu_2(\mu_2\text{-}1,1\text{-}N_3)_2$ cores have been observed in, for example, $[Cu_2(OBISDIEN)(\mu_2\text{-}N_3)_2(N_3)_2]\cdot H_2O$ [18] and $[Cu_2(t\text{-}Bupy)_4(\mu_2\text{-}N_3)_2](ClO_4)_2$,[20] and in the majority of cases the four-membered $Cu_2N_2$ cores are planar. In contrast, the dihedral angle of 153° between the Cu(1)/N(1)/N(4) and Cu(2)/N(1)/N(4) planes in **4** indicates a "roof-shaped" geometry similar to that observed for the $Cu_2O_2$ cores in **2** and **3**. The Cu···Cu separation in **4** [3.006(5) Å] is thus slightly shorter than that found in the two azido-bridged complexes mentioned above [3.162(1) and 3.042(3) Å]. The cross-durene ring distances and internuclear distances are quite long, as was the case for **1** and **2**. The Cu−N−Cu angles are very similar [98.1(4) vs 96.6(4)°], but there are small variations in the Cu−N(azido) bond lengths [1.970(9) − 2.03(1) Å]. The azido ligands in **4** are essentially linear, with $N_\alpha-N_\beta-N_\gamma$ angles of 179(1)°. The $N_\alpha-N_\beta$ bonds [1.19(1) and 1.20(1) Å] are slightly longer than the $N_\beta-N_\gamma$ bonds [1.13(1) and 1.14(2) Å], with the longer bond involving the nitrogen ($N_\alpha$) coordinated to the Cu(II) centers. Similar differences in bond lengths have been noted for azido ligands coordinating in a terminal or $\mu$-1,1 bridging fashion.[18,20,21]

It may have been anticipated that, given the large metal−metal separations observed for the nonbridged Cu(II) complex of $L^{dur}$, **1**, the azido-bridged complex would prefer the $\mu$-1,3 end-to-end coordination mode. However, as Peacock,[37] Tolman,[38] and their co-workers have previously demonstrated, tacn derivatives which are linked at meta positions on an aromatic ring can indeed support single atom bridges between two metal centers.

**Magnetic Susceptibility Studies.** The general interest in the magnetism of hydroxo-, alkoxo-, and azido-bridged Cu(II) complexes and the fact that complexes **2**−**4** have unusual "roof-shaped" $Cu_2X_2$ geometries, indicated that an investigation of their magnetic properties was warranted. Variable-temperature magnetic susceptibility measurements were carried out on powdered samples of the bridged complexes in the 4.2−300 K temperature range. The plots of magnetic moment ($\mu_{eff}$) and magnetic susceptibility ($\chi_M$) versus temperature are shown in Figures 5.

The magnetic susceptibilities of four samples of **2** were measured, and the results were all similar. They show a gradual increase with decreasing temperature, reaching a maximum at 40 K and then decrease to a minimum at 28 K (Figure 5a). Below this temperature, $\chi_M$ increases again due to the presence of a paramagnetic impurity, the exact nature of which is not known. The maximum at ∼40 K is indicative of weak antiferromagnetic coupling occurring between the Cu(II) centers in the $Cu_2X_2$ moieties. The corresponding plot of magnetic moment [per Cu(II) center] vs temperature shows a decrease from 1.69 $\mu_B$ at 300 K to 0.54 $\mu_B$ at 4.2 K.

The data for **2** were fitted to eq 1, which models the complex as a pair of independent Cu(II) dimers.

$$\chi_M = (1 - x)(N\beta^2g^2/kT)[3 + \exp(-2J/kT)]^{-1} + xN\beta^2g^2/4kT + N\alpha \quad (1)$$

(38) Tolman, W. B. *Acc. Chem. Res.* **1997**, *30*, 139. Mahapatra, S.; Kaderli, S.; Llobet, A, Neuhold, Y.-M.; Palanch, T.; Halfen, J. A.; Young, V. G., Jr.; Kaden, T. A.; Que, L., Jr.; Zuberbühler, A. D.; Tolman W. R. *Inorg. Chem.* **1997**, *36*, 6343 and references therein.

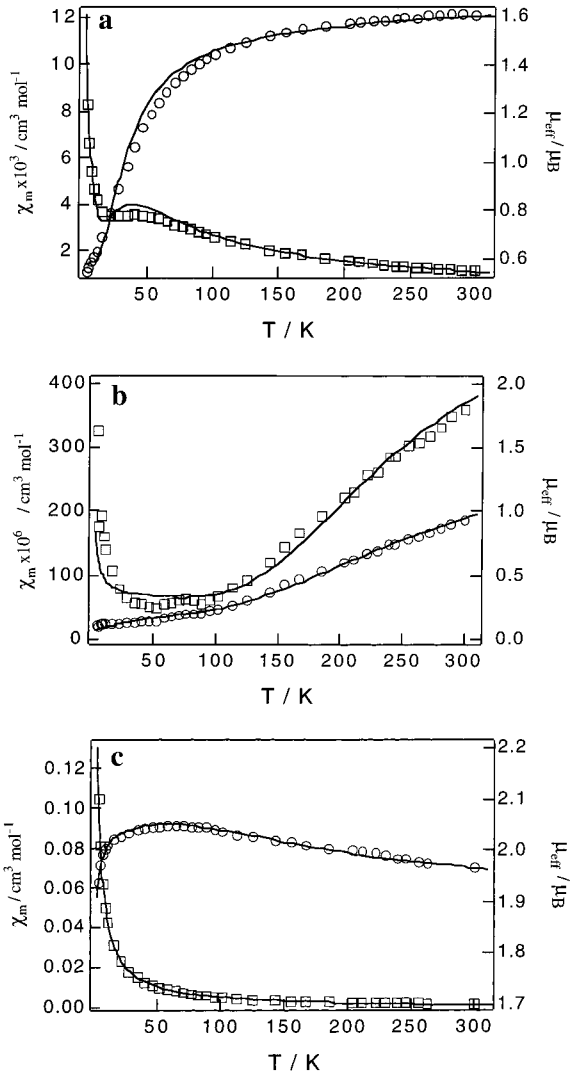


**Figure 5.** Plot of $\chi_M$ (□) and $\mu_{eff}$ (○) (per Cu) versus temperature for **2** (a), **3** (b), and **4** (c). Solid lines show the best-fits to eq 1 yielding the following: for **2**, $g = 1.85$, $J = -27$ cm$^{-1}$, $x = 0.13$, $N\alpha = 60 \times 10^{-6}$ cm$^3$ mol$^{-1}$; for **3**, $g = 2.0$, $J = -269$ cm$^{-1}$, $x = 0.001$, $N\alpha = 60 \times 10^{-6}$ cm$^3$ mol$^{-1}$; for **4**, $g = 2.06$, $J = 94$ cm$^{-1}$, $\Theta = -0.56$ K, $N\alpha = 64 \times 10^{-6}$ cm$^3$ mol$^{-1}$.

The first (Bleaney−Bowers) term accounts for the di-$\mu_2$-hydroxo-bridged Cu(II) pairs. A Curie term was introduced to allow for a fraction ($x$) of paramagnetic impurity, and $\chi_M$ is expressed per mole of Cu(II). The parameters $N$, $\beta$, and $k$ in eq 1 have their usual meanings, and $N\alpha$ is the temperature-independent paramagnetism. The least-squares fit of eq 1 to the data yielded the parameters $g = 1.85$, $J = -27$ cm$^{-1}$, $x = 0.13$, and $N\alpha = 60 \times 10^{-6}$ cm$^3$ mol$^{-1}$. The value of $J$ reveals weak antiferromagnetic interaction between the Cu(II) ions within the $Cu_2(\mu\text{-}OH)_2$ moieties. The fit is generally good except in the region of $\chi_{max}$, as noted in previous work.[40] The low value of $g$ is most likely indicative of dimer−dimer interactions involving neighboring $[Cu_4L^{dur}(\mu_2\text{-}OH)_4]^{4+}$ ions. It could also result from some of the more strongly coupled complex, **3**, being present (see below and synthetic details in Experimental Section), which would lower $\chi_{Cu}$ and, hence, the $g$ value. Fixing of the $g$ value to 2.0 led to a poorer fit and crossing of the observed and calculated data.

As indicated earlier, studies of di-$\mu_2$-hydroxo-bridged Cu(II) dimers have been pivotal in the development of structure−magnetism correlations.[4,41] Experimentally, Crawford et al. [4] found that for dimers with planar or near-planar $[Cu_2(\mu_2\text{-}OH)_2]^{2+}$ cores, the exchange constant ($J$) varies linearly with the Cu−O−Cu angle ($\theta$), $2J = -74.53\theta + 7270$ cm$^{-1}$. Thus the interaction is predicted to be antiferromagnetic ($S = 0$ ground state) for $\theta > 97.5°$ and ferromagnetic ($S = 1$ ground state) for $\theta < 97.5°$. Application of a molecular orbital exchange model focusing on the antiferromagnetic contribution to $J$ ($=J_{AF} + J_F$) led to the view that interaction of the magnetic $d_{xy}$ orbitals in the Cu(II) centers results in asymmetric and symmetric molecular orbitals, $\Psi_A$ and $\Psi_S$, with energies, $\epsilon_A$ and $\epsilon_S$, dependent on the metal−oxygen overlaps, $S_x = |\langle d_{xy}|2p_x\rangle|$ and $S_y = |\langle d_{xy}|2p_y\rangle|$, respectively. For $\theta > 90°$, $S_x > S_y$, while for $\theta < 90°$, the opposite is true. Thus, for $\theta \gg 90°$, the energy gap, $\Delta = \epsilon_A - \epsilon_S$, is large, leading to a preponderant antiferromagnetic contribution to $J$, since this is proportional to $\Delta^2$.[41−43] As $\theta$ is reduced toward 90°, $\Delta$ becomes smaller and the contribution of $J_{AF}$ to $J$ diminishes.

Other angular distortions to the $LCu(\mu_2\text{-}OH)_2CuL$ unit may also attenuate the value of $J$. For example, the magnetic interaction becomes less antiferromagnetic at a given value of $\theta$ as the dihedral angle ($\delta$) between the two $Cu_2O$ planes is reduced from 180°.[5] Bending of the $Cu_2O_2$ core causes a decrease in the $S_x$ overlap (and hence $\epsilon_A$), while the $S_y$ overlap (and $\epsilon_S$) remain unchanged. Since $\epsilon_A$ is above $\epsilon_S$, the result is a decrease in $\Delta$ and $J_{AF}$.

The listing of selected structural and magnetic data for complex **2** and for a number of related complexes in Table 5 indicates that there is no simple direct correlation between the values of $J$ and the corresponding $\delta$ values. This is due to the significant variation in $\theta$, the Cu−O−Cu angles, and the degree of asymmetry of the bent cores (highlighted by the two different $\theta$ values). Notably, the $J$ value for $[Cu_2(C_6H_{11}NH_2)_4(\mu_2\text{-}OH)_2](ClO_4)_2$ is significantly more negative than that determined for **2**, despite the similar $\delta$ angles for these compounds, and the weakest antiferromagnetic interaction is associated with $[Cu_2(CH_3NH_2)_4(\mu_2\text{-}OH)_2](SO_4)\cdot H_2O$, which has the smallest dihedral angle. The weaker exchange coupling supported by the bent $[Cu_2(\mu_2\text{-}OH)_2]^{2+}$ cores in **2**, compared with than found for $[Cu_2L^{mx}(\mu_2\text{-}OH)_2](BPh_4)_2$ (flat core), is nonetheless consistent with the significantly smaller $\delta$ angle observed in **2**.

The observed and calculated susceptibility data for the methoxo-bridged complex **3** are shown in Figure 5b. The best-fit parameters of $J = -269$ cm$^{-1}$ $g = 2.0$, $N\alpha = 60 \times 10^{-6}$ cm$^3$ mol$^{-1}$, and $x = 0.001$ are indicative of strong antiferromagnetic coupling, $J$ being similar in size to those of related di-$\mu$-alkoxo-bridged complexes with similar $\delta$ and Cu···Cu values (see Table 5).

Figure 5c shows the temperature dependence of the magnetic susceptibility and magnetic moment for the azido-bridged complex, **4**, over the temperature range 300−4.2 K. The magnetic moment of 1.98 $\mu_B$ at 300 K is higher than that observed for the nonexogenously bridged tetranuclear complex, $[Cu_4L^{dur}(H_2O)_8](ClO_4)_8\cdot 9H_2O$ (1.85 $\mu_B$), and shows a steady increase with decreasing temperature, reaching a maximum of 2.05 $\mu_B$ at 65 K. This behavior is indicative of ferromagnetic

(39) Handa, M.; Idehara, T.; Nakano, K.; Kasuga, K.; Mikuriya, M.; Matsumoto, N.; Kodera, M.; Kida, S. *Bull. Chem. Soc. Jpn.* **1992**, *65*, 3241.
(40) Mazurek, W.; Berry, K. J.; Murray, K. S.; O'Connor, M. J.; Snow, M. R.; Wedd, A. D. *Inorg. Chem.* **1982**, *21*, 3071.
(41) Kahn, O. *Molecular Magnetism*; VCH: Weinheim, Germany, 1993.
(42) Kahn, O.; Briat, B.; Galy, J. *J. Chem. Soc., Dalton Trans.* **1977**, 1453.
(43) Hay, P. J.; Thibeault, J. C.; Hoffman, R. *J. Am. Chem. Soc.* **1975**, *97*, 4884.

coupling. Below 50 K, the magnetic moment decreases, which could be due to the combined effects of zero-field splitting of the triplet ground state and intermolecular antiferromagnetic interactions. Owing to the large separation between the two pairs of azido-bridged Cu(II) centers in **4**, the data were analyzed using eq 1, which models the complex as a pair of magnetically independent dimers. A Weiss constant ($\Theta$) was introduced into the temperature term to account for both intermolecular effects and zero-field splitting. The best-fit parameters were $g = 2.06$, $J = 94$ cm$^{-1}$, $\Theta = -0.56$ K, and $N\alpha = 64 \times 10^{-6}$ cm$^3$ mol$^{-1}$. A fraction of monomeric impurity, *x*, was not required in order to obtain the best-fit, but there is some evidence for its presence from EPR spectroscopy (see below). The *J* value indicates moderately strong ferromagnetic interaction between the pairs of azido-bridged Cu(II) centers. The data in Figure 5c are similar to those of $[Cu_2(t\text{-Bupy})_4(\mu_2\text{-}N_3)_2](ClO_4)_2$ for which $g = 2.17$, $J = 53$ cm$^{-1}$, $\Theta = -0.57$ K, and $N\alpha = 0$ cm$^3$ mol$^{-1}$. [20]

The azide ligand generally mediates a ferromagnetic interaction between Cu(II) centers when bound in a $\mu_2$-1,1 end-on fashion and antiferromagnetic coupling when bridging in a $\mu_2$-1,3 end-to-end mode. Kahn and co-workers[28] and Ruiz et al.[29] have examined a "spin-polarization" model for azido-mediated coupling in which the two opposite spins in the highest occupied molecular orbital ($\pi_g$) of the azide ligand are localized at the terminal nitrogen atoms of the ligand. For the $\mu_2$-1,1 bridging mode, simultaneous pairing of the two Cu(II) spins with the opposite spin of the bridging nitrogen would then result in ferromagnetic coupling between the two Cu(II) spins, irrespective of the value of the azide bridge angle ($\theta$). Recently, however, Thompson and co-workers[23,25] have noted some limitations of this model, reporting a number of dicopper(II) complexes with diazine/$\mu_2$-1,1-azido bridges which indicate that $\mu_2$-1,1-azide bridges can propagate antiferromagnetic interaction if $\theta > 108.5°$. A polarized neutron diffraction study of $[Cu_2(t\text{-Bupy})_4(\mu_2\text{-}N_3)_2](ClO_4)_2$ found that the spins of the bridging azide nitrogens are the same sign as those of the Cu(II) centers.[28] The observation that azide propagates ferromagnetic coupling at bridging angles for which an hydroxide mediates strong antiferromagnetic interaction may be rationalized in terms of the lower electronegativity of the azide ligand. Due to a decrease in the energy separation between the s valence orbitals of the bridge and the $d_{xy}$ orbitals of the Cu(II) centers, the $\Psi_S$ orbital is destabilized with respect to the $\Psi_A$ orbital. The relatively small $\Delta$ value in the range of $\theta = 90-110°$ means that the $J_{AF}$ contribution to *J* is reduced and the $J_F$ term dominates.

In light of this discussion, it is not surprising that **4** displays ferromagnetic coupling, while the hydroxo-bridged complex **2** with similar bridging angles shows antiferromagnetic behavior. Table 5 compares the magnetic and structural data of **4** with other reported bis($\mu_2$-1,1-azido)copper(II) complexes. The weakest ferromagnetic coupling is observed for $[Cu_2(OBISDIEN)(\mu_2\text{-}N_3)_2(N_3)_2]\cdot H_2O$, which contains a planar core with the largest average Cu−N−Cu angle and Cu···Cu separation. The strongest ferromagnetic coupling is observed in the complexes with bent geometries, namely **4** and $[Cu_2(DMPTD)_4(\mu_2\text{-}N_3)_2(N_3)_2]$. Indeed, **4** exhibits the highest *J* value reported to date for a bis($\mu_2$-1,1-azido)copper(II) complex, consistent with the fact that this complex features the smallest average Cu−N−Cu angle and Cu···Cu separation.

**Electron Spin Resonance Spectra of 4.** The ESR spectra of neat powdered samples of the azido-bridged complex, **4**, were measured at temperatures of 6−290 K and frequencies of 33.9 GHz (Q-band) and 90 GHz. The main aim was to confirm the $S = 1$ ground state per $Cu_2$ moiety by observing the triplet state lines.[44] These are indeed evident as $\Delta M_S = 1$ transitions in the 120 K Q-band spectrum at 4500 G and 17 000 G (Figure 6). The line at ~11 000 G ($g = 2.1$) may originate from monomer impurity or from inter-tetranuclear effects, the former being more likely in view of the $A_{||}$ hyperfine splitting of 250 G observed in the frozen MeCN/toluene spectrum at 118 K. Since the triplet state lines remain in the frozen solution spectrum, the $\mu$-$N_3$-dinuclear species must therefore be retained in solution. Temperature variation of the powder spectra (Supporting Information) revealed a gradual increase in the intensity of the 4500 and 17 000 G resonances between 120 and 10 K, as anticipated for the increased thermal population of the $S = 1$ ground state. The line at 11 000 G also increases in intensity as the temperature is lowered. Measurements of the neat powder of **4** made at 90 GHz confirm the triplet state spectrum with lines at ca. 2.5, 3.2, and 3.5 T. Weak lines at ~1.5 T are probably "forbidden" $\Delta M_S = 2$ transitions.[44] Sikorav et al.[20] have previously reported the X-band triplet-state ESR spectrum of $[Cu_2(t\text{-Bupy})_4(\mu_2\text{-}N_3)_2](ClO_4)_2$, at $T = 4.2$ K. On warming of the sample to room temperature, the lines diminish in intensity leaving only a signal due to monomer impurity. This contrasts with the spectra of **4** in which triplet state lines persist at 290 K.

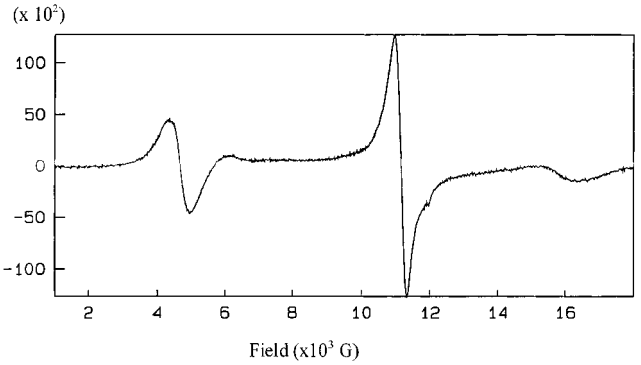


**Figure 6.** Q-band (33.89 GHz) ESR spectrum of a neat powdered sample of **4** measured at 120 K. (See the Experimental Section for instrument settings.)

## Conclusion

This work demonstrates that the attachment of four 1,4,7-triazacyclononane macrocycles to a durene backbone generates a ligand assembly capable of supporting bridged polynuclear complexes with uncommon bridging core geometries and interesting magnetic behavior. Such ligands, therefore, provide an opportunity to further develop correlations between magnetic properties and molecular structure.

**Acknowledgment.** This work was supported by grants from the Australian Research Council. B.G. was the recipient of an Australian Postgraduate Award.

**Supporting Information Available:** Three X-ray crystallographic files in CIF format and a figure showing the temperature dependence of Q-band ESR spectra for a neat powdered sample of **4** (Figure S1). This material is available free of charge via the Internet at http://pubs.acs.org.

IC000991H

(44) Smith T. D.; Pilbrow, J. *Coord. Chem. Rev.* **1974**, *13*, 173.